Nanoscale detection of organic signatures in carbonate microbialites

Karim Benzerara[†‡§], Nicolas Menguy[†], Purificación López-García[¶], Tae-Hyun Yoon[‡‖], Józef Kazmierczak[††], Tolek Tyliszczak[‡‡], François Guyot[†], and Gordon E. Brown, Jr.[‡§§]

[†]Institut de Minéralogie et de Physique des Milieux Condensés, Unité Mixte de Recherche 7590, Centre National de la Recherche Scientifique, Department de Minéralogie, Institut de Physique du Globe de Paris, University of Paris 6 and 7, 140 Rue de Lourmel, 75015 Paris, France; [‡]Surface and Aqueous Geochemistry Group, Department of Geological and Environmental Sciences, Stanford University, Stanford, CA 94305-2115; [¶]Unité d'Ecologie, Systématique et Evolution, Unité Mixte de Recherche 8079, Centre National de la Recherche Scientifique, Université Paris-Sud, 91405 Orsay Cedex, France; [‖]Department of Chemistry, Hanyang University, Music 17 Haengdang-dong, Seongdong-gu, Seoul, 133-791, Korea; [††]Institute of Paleobiology, Polish Academy of Sciences, Twarda 51/55, 00818 Warsaw, Poland; [‡‡]Advanced Light Source, Lawrence Berkeley National Laboratory, Berkeley, CA 94720; and [§§]Stanford Synchrotron Radiation Laboratory, Stanford Linear Accelerator Center, MS 69, 2575 Sand Hill Road, Menlo Park, CA 94025

Communicated by W. G. Ernst, Stanford University, Stanford, CA, April 21, 2006 (received for review January 12, 2006)

Microbialites are sedimentary deposits associated with microbial mat communities and are thought to be evidence of some of the oldest life on Earth. Despite extensive studies of such deposits, little is known about the role of microorganisms in their formation. In addition, unambiguous criteria proving their biogenicity have yet to be established. In this study, we characterize modern calcareous microbialites from the alkaline Lake Van, Turkey, at the nanometer scale by combining x-ray and electron microscopies. We describe a simple way to locate microorganisms entombed in calcium carbonate precipitates by probing aromatic carbon functional groups and peptide bonds. Near-edge x-ray absorption fine structure spectra at the C and N K-edges provide unique signatures for microbes. Aragonite crystals, which range in size from 30 to 100 nm, comprise the largest part of the microbialites. These crystals are surrounded by a 10-nm-thick amorphous calcium carbonate layer containing organic molecules and are embedded in an organic matrix, likely consisting of polysaccharides, which helps explain the unusual sizes and shapes of these crystals. These results provide biosignatures for these deposits and suggest that microbial organisms significantly impacted the mineralogy of Lake Van carbonates.

aragonite | biosignature | biomineralization | spectromicroscopy

Lake Van (eastern Anatolia, Turkey) is the largest soda lake on Earth, with a pH of 9.7–9.8 and a salinity of 21.7‰ (1). It harbors the largest known living microbialites, which are structures resulting from precipitation of aragonite at sites where calcium-rich groundwater seeps into the alkaline lake water (1, 2) and are associated with a wide diversity of microorganisms (3). Lake Van microbialites have a fine-grained micritic texture similar to most carbonate microbialites (4, 5) and consist of 30- to 100-nm-sized aragonite crystals (2, 3), which have morphologies that resemble bacteria-like forms (2). Some authors have suggested the possibility that nanospheres in microbialites could represent very small, entombed bacteria or "nanobacteria" (4, 5). However, the real nature of these carbonates, as well as their relationship to the microorganisms detected in the microbialites, remain unresolved.

Because Lake Van is highly oversaturated with aragonite (1), the role of microorganisms in aragonite precipitation can be questioned, and the observed presence of microbes in these structures could simply result from passive trapping during mineral precipitation. This question is not new and has been raised systematically since the earliest studies of microbialites to the most recent ones (e.g., refs. 6–9). Some studies have demonstrated that microbes can actively mediate carbonate, in particular dolomite, precipitation (10). However, if passive trapping is operative, features suggesting that discrimination between microbially generated and purely abiotic precipitates is possible may be illusory. For example, the biogenicity of ancient stromatolites (i.e., laminated microbialites), usually considered as evidence of some of the oldest life on Earth, has been thoroughly questioned because the macroscopic structure of stromatolites does not constitute a biosignature, and no unambiguous evidence for fossilized microbes has been found in most

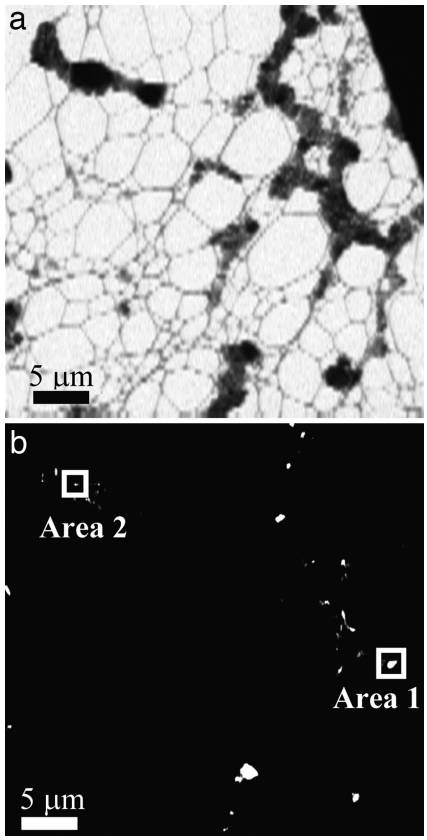

Fig. 1. STXM images of Lake Van microbialites. (*a*) Image of microbialites at 288.2 eV. Image is 4 μm $\times$ 40 μm. (*b*) Map of peptide-rich areas absorbing at 288.2 eV showing a number of bright spots of various morphologies. Area 1 and area 2 correspond to bright spots that were further analyzed in Figs. 2 and 4, respectively.

Conflict of interest statement: No conflicts declared.

Abbreviations: ACC, amorphous calcium carbonate; EELS, electron energy loss spectroscopy; EPS, extracellular polymeric substances; NEXAFS, near-edge x-ray absorption fine structure; STXM, scanning transmission x-ray microscopy; TEM, transmission electron microscopy.

[§]To whom correspondence should be addressed. E-mail: benzerar@impmc.jussieu.fr.

www.pnas.org/cgi/doi/10.1073/pnas.0603255103

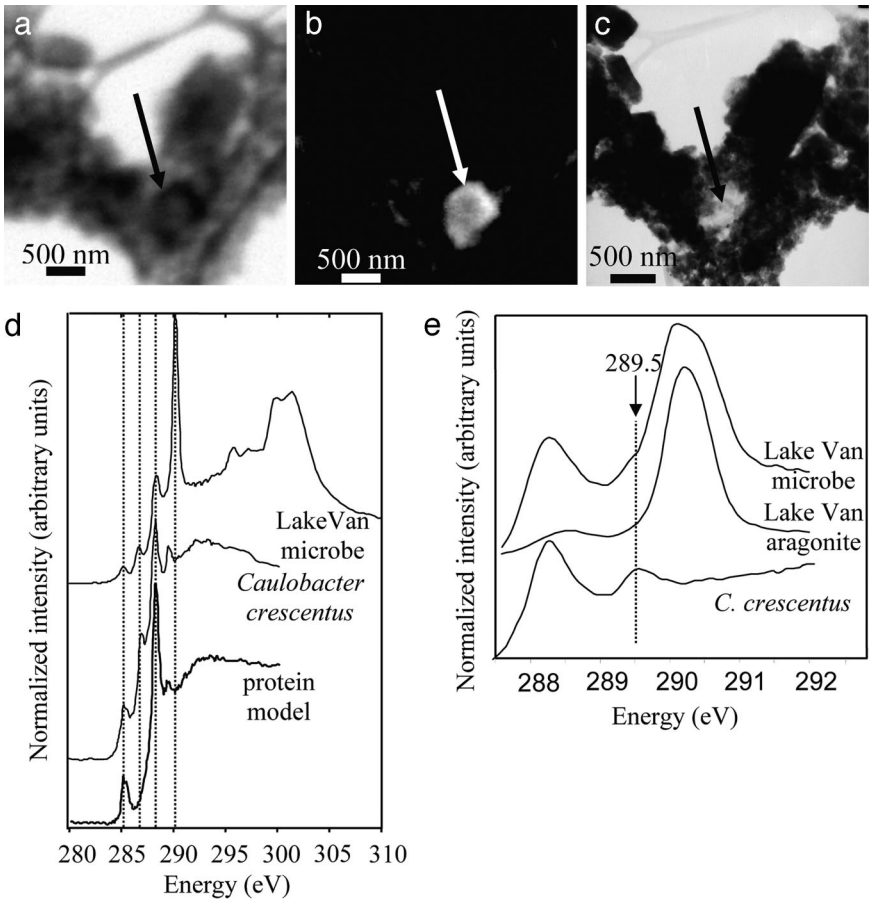

Fig. 2. Spectromicroscopy analysis of Lake Van microorganisms. (*a*) STXM image at 288.2 eV of area 1 (see Fig. 1). The arrow indicates a protein-rich area. (*b*) Equivalent map of objects absorbing at 288.2 eV. (*c*) TEM image of the same area. The protein-rich area displays a low contrast compared with the surrounding aragonite. (*d*) C K-edge NEXAFS spectra from the protein-rich area (Lake Van microbe), reference *C. crescentus* cells, and albumin as a protein model compound. Dashed lines at 285.2, 286.8, and 288.2 eV highlight the prevalent peaks observed in the Lake Van microbe and *C. crescentus*. The dashed line at 290.2 eV highlights the carbonate peak. (*e*) Close-up of the C K-edge NEXAFS spectra of the protein-rich area in the Lake Van microbialite, Lake Van aragonite, and *C. crescentus* in the 287.5- to 292-eV energy range. The arrow indicates the position of a shoulder at 289.5 eV.

of them (11, 12). A major problem hampering this type of study is recognition of microorganisms in a highly mineralized, fine-grained matrix. Optical and scanning electron microscopies are frequently used for studying microbialites, but they provide only morphological and compositional information, which cannot be used to reliably discriminate between fossilized microbes and calcium carbonate crystals. Lake Van microbialites are associated with a wide diversity of contemporary cyanobacteria and alkaliphilic and/or heterotrophic bacteria (3). Locating these microorganisms by conventional or epifluorescent optical microscopy is difficult, however, because of the high relief of aragonite crystals relative to microorganisms, the small size of the latter, and the difficulty in distinguishing the fluorescence signal of aragonite crystals from that of stained cells. To overcome these problems and to explore the association between minerals and organic molecules comprising the Lake Van microbialites, we combined scanning transmission x-ray microscopy (STXM) (13), which allows imaging and acquisition of near-edge x-ray absorption fine structure (NEXAFS) spectra at high spectral and spatial resolution, and transmission electron microscopy (TEM) (14), on the same samples. Our observations show the intimate association of polysaccharides with the mineral matrix at the nanoscale and strongly suggest that microbial organisms played an important role in the formation of the Lake Van microbialites.

Results

As described below, STXM provided strong evidence for the presence of microbial cells in the Van Lake microbialites in the form of organic functional groups typically associated with microorganisms. Those areas identified as microorganisms always contained peptide bonds characterized by a specific absorption feature in the carbon K-edge at 288.2 eV. In contrast, the surrounding carbonates displayed a strong absorption peak at 290.2 eV (13). Taking into account these spectroscopic differences, energy-filtered imaging was used to map proteins in the carbonate microbialites (Fig. 1). Bright spots were observed (Fig. 1*b*) with filamentous or spherical morphologies and diverse sizes in the submicrometer to micrometer size range compatible with those of individual microbial cells (15) or remnants of microbial cells. Reference microorganisms [the Gram-negative *Caulobacter crescentus* (α-Proteobacteria) and the Gram-positive *Bacillus subtilis* (see Fig. 6, which is published as supporting information on the PNAS web site), but also the γ-Proteobacterium *Shewanella oneidensis*, the cyanobacterium *Synechococcus leopoliensis*, or the β-Proteobacterium *Ramlibacter tataouinensis* (data not shown)] all displayed identical complex NEXAFS spectra at the carbon K-edge, dominated by the specific absorption of proteins at 288.2 eV (13, 16) (Fig. 6). The similarity of NEXAFS spectra at the carbon K-edge for diverse bacteria basically results from the universal basic chemistry of living cells, all of which contain proteins, polysaccharides,

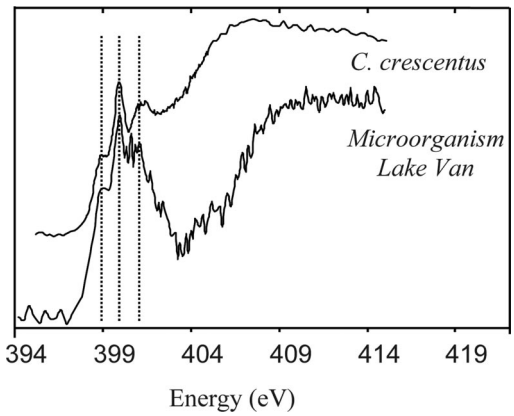

Fig. 3. Nitrogen K-edge NEXAFS spectra of Lake Van calcified microorganisms. The energy positions of the peaks are, respectively, 399, 399.9, and 401.2 eV.

and nucleic acids. Therefore, no major differences are expected for the other microbial groups that have not yet been investigated. Based on both morphological and spectroscopic considerations, we argue that the peptide-bond map of Lake Van microbialite samples shows the locations of living or fossilized microbial cells. In addition to the peptide peak at 288.2 eV, peaks at 285.2 and 286.8 eV were observed that correspond, respectively, to aromatic groups (16) and phenolic or ketonic groups, all of which were observed in C K-edge NEXAFS spectra of the reference bacteria in similar ratios (Fig. 2; and see Figs. 6–8, which are published as supporting information on the PNAS web site). The systematic presence of a carbonate peak at 290.2 eV in the C K-edge NEXAFS spectrum of the peptide-, aromatic-, and ketone-rich regions of the Lake Van microorganisms indicates that they are closely associated with carbonates (Fig. 2). In addition, the carbonate peak overlaps a peak at 289.5 eV, which was detected systematically and exclusively in those regions (Fig. 2). The energy position of this peak matches the peak observed in reference bacterial cells and in nucleic acids (13, 17). Hence, these regions have a complex spectrum identical to those of diverse cultured bacterial strains, which strongly supports the identification of the observed spots within the Lake Van carbonates as microbial cells. The detection of microorganisms was further supported by spectroscopy at the N K-edge, which showed the presence of nitrogen associated with protein-rich areas, with a spectroscopic signature very similar to that observed in *C. crescentus* cells (Fig. 3). Peaks at 399 and 399.9 eV are related to heterocyclic aromatics such as pyridine (18), which are present in many biological molecules (e.g., nucleic acids, ATP). The peak at 401.2 eV is related to amide groups (19). Therefore, spectromicroscopy allowed the detection of living and/or fossilized microorganisms in microbialites by characterizing and mapping, within a mineral matrix, organic functional groups composing microbial cells. These cell-shaped areas rich in peptide bonds, phenolic/ketonic and aromatic groups, and organic nitrogen were systematically located and imaged by TEM. However, in most of the samples examined, microbial cells

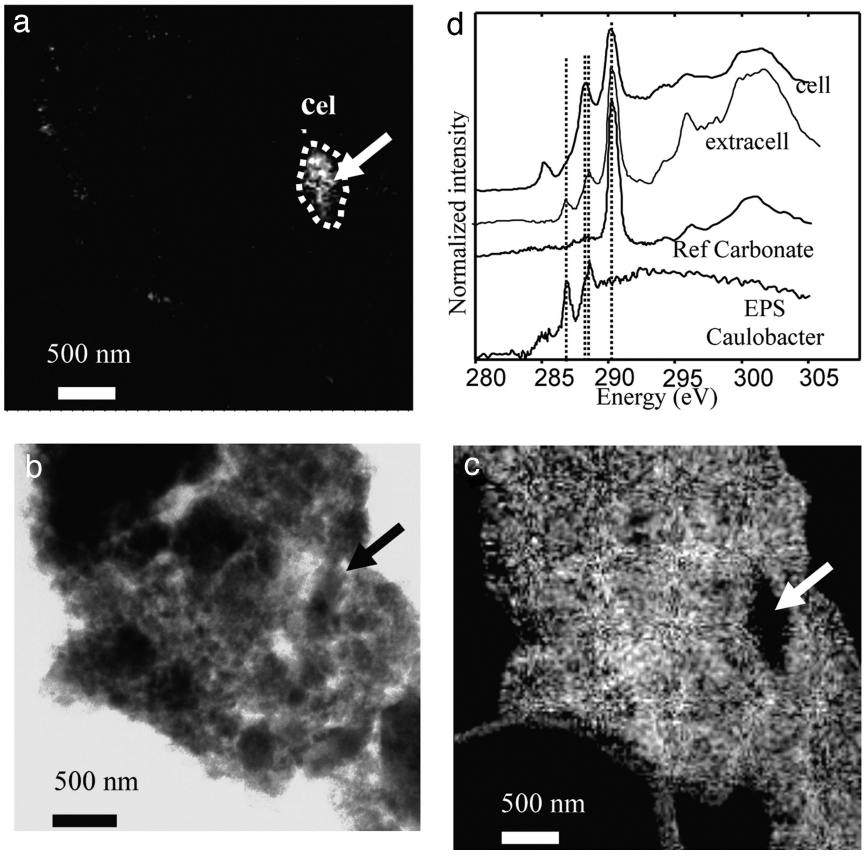

Fig. 4. Spectromicroscopy analyses of Lake Van aragonite micrite (see area 2 in Fig. 1). (*a*) STXM map of peptides taken at 288.2 eV showing the presence of a microbial cell (outline and arrow). (*b*) TEM image of the same area. The major part of this area is a cluster of aragonite nanospheres not visible at this magnification. The arrow shows the same location as in *a*. (*c*) STXM map of carbon-containing molecules absorbing specifically at 288.6 eV. (*d*) C K-edge NEXAFS spectra from the microbial cell seen in *a*, from the surrounding aragonite (extracell), and from reference calcium carbonate and *C. crescentus* EPS. Dashed lines at 286.8 eV, 288.2 eV, 288.6 eV, and 290.2 eV highlight peaks observed in the calcified microorganisms, the Lake Van aragonite matrix, and *C. crescentus* EPS.

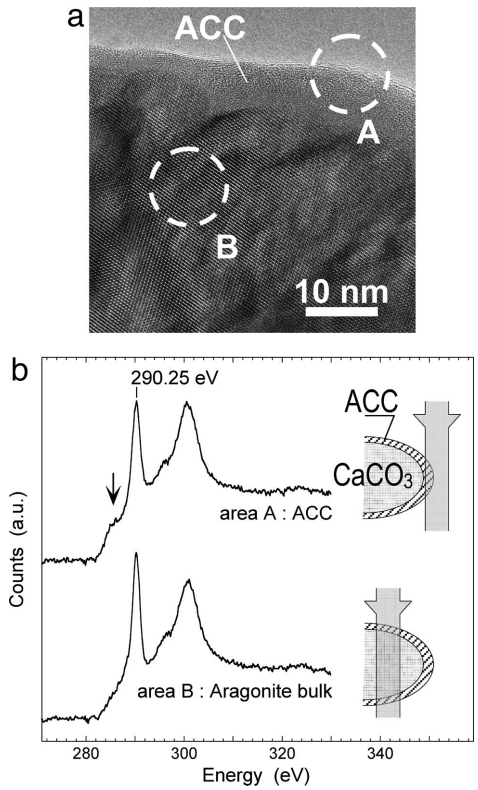

Fig. 5. TEM observation of Lake Van aragonite nanocrystals. (*a*) HRTEM image of an aragonite crystal along the [1–11] zone axis. The presence of lattice fringes in the interior of the aragonite indicates that this region is crystalline, and their absence in the edge region indicates an amorphous outer layer. (*b*) EELS spectra of the crystallized inner part (area B) versus the amorphous outer layer (area A). (*Insets*) Schematic views of the electron beam path through an aragonite nanoglobule for areas A and B. Area A contains only the ACC layer, whereas area B contains mostly aragonite and a small fraction of ACC. The arrow shows a peak at 287 eV observed in spectrum of the ACC layer, which is more poorly resolved in the spectrum of bulk aragonite.

were masked in the TEM images by strongly diffracting aragonite nanoglobules precipitated on them (Figs. 4 and 8).

In addition to microbial cells with highly localized distribution, a second type of organic component showed a much wider distribution in Lake Van microbialites. Most of the samples examined, other than in the peptide-rich regions, consisted of clusters of aragonite nanospheres visible by TEM (3) (Fig. 4). Although spectromicroscopy on those clusters showed no aromatic groups (285.2 eV) or peptide bonds (288.2 eV), peaks at 286.8 and 288.6 eV were detected together with the main carbonate peak at 290.2 eV (Fig. 4). The peaks at 286.8 and 288.6 eV, which were absent in C K-edge NEXAFS reference spectra of abiotic aragonite crystals, corresponded to ketone and carboxylic groups, respectively. They are also observed in acidic polysaccharides (17) and in extracellular polymeric substances (EPS) from *C. crescentus* (Fig. 4), suggesting that similar polysaccharides were associated with Lake Van aragonite nanocrystals. Such polymers were observed throughout the carbonate clusters at a spatial scale down to a few tens of nanometers (Fig. 4). Epifluorescence microscopy observations were performed on Lake Van microbialites by using the fluorescently labeled lectin Con A, which has high affinity for α-D-mannose and α-D-glucose residues and has been validated and extensively used in previous studies on carbonate microbialites to probe mannose and/or glucose residues at nonreducing terminals of polysaccharides (17, 20–21). They support our spectromicroscopy observations by suggesting the presence of these polymers throughout Lake Van carbonates at a larger scale (see Fig. 9, which is published as supporting information on the PNAS web site). The validity of the spectroscopic signatures proposed for calcified cells and EPS in the Lake Van microbialites was checked on 4-year-old experimentally calcified bacterial biofilms consisting of the β-Proteobacterium *R. tataouinensis*. STXM observations showed the presence, in the experimentally calcified cultures, of *R. tataouinensis* cells displaying C K-edge and N K-edge NEXAFS spectra identical to those from Lake Van microbial cells and extracellular polymers with C K-edge NEXAFS spectra identical to Lake Van EPS (see Fig. 10, which is published as supporting information on the PNAS web site).

In addition to the presence of localized protein signatures and of widespread polysaccharides in the microbialites, the Lake Van microbialite aragonite crystals display other remarkable features, which suggest growth in the presence of organic molecules. High-resolution TEM showed that each nanosphere, previously interpreted as "nanobacteria" (2), is a single crystal of aragonite surrounded by a few-nanometer-thick layer of amorphous calcium carbonate (ACC) (Fig. 5; and see Fig. 11, which is published as supporting information on the PNAS web site). Electron energy loss spectroscopy (EELS) spectra at the C K-edge of Lake Van ACC layers show a broad peak around 287 eV (Fig. 5). These EELS data are comparable with those obtained in two previous studies, one on natural calcite crystal clusters associated with a polysaccharidic matrix (14) and one on cultures of cyanobacteria mediating calcite precipitation (22). Based on the C K-edge NEXAFS data obtained by STXM analysis on the same sample, we propose that the ACC layer surrounding the aragonite crystals contains polysaccharide-like molecules.

Discussion

Our results show the presence of an intricate nanometer-scale mixture of organic molecules and calcium carbonate crystals in recent microbialites. They also highlight the advantage of using STXM to look for microbes in carbonate micrite, because fossilized or carbonate-covered microbes are extremely difficult to recognize by electron microscopy alone (Fig. 4). Hence, the combination of STXM with HRTEM provides a unique means of detecting microbial cells in such complex samples. The microbial cells observed in this study by STXM mapping of proteins do not display perfect cell shapes (see Figs. 2 and 4). In addition to the methodological difficulty in mapping cell shapes with high precision in a mineral matrix based on specific spectroscopic features, the lack of well defined cellular morphologies may also result from the well documented lyses damage that occurs during fossilization, altering microbe morphologies (e.g., refs. 23–25). The diverse morphologies and sizes of microbial cells we observed in Lake Van microbialites are, however, not consistent with only cyanobacteria but suggest a large diversity of heterotrophs as evidenced by molecular genetic surveys of the same samples (3). Cyanobacteria are commonly believed to be the best preserved fossils and to have played a major role in the formation of some present and past carbonate microbial deposits (e.g., ref. 26), including microbialites (8). This belief, however, is strongly biased by the fact that cyanobacterial morphologies are among the most easily recognized prokaryotic types (27).

Our observations have major implications for understanding microbially induced carbonate formation. Although the pervasive presence of EPS in microbialites and their importance in the formation of microbial carbonates has been noted by many previous studies (e.g., refs. 28–34), how EPS are involved in carbonate precipitation is still a matter of intense debate. ACC is a highly unstable phase but can be stabilized in the presence of a variety of organic or inorganic additives (35). Similar to what has been noticed for other microbialites (e.g., ref. 4), the morphology of Lake Van aragonite crystals is unusual compared with the morphology of crystals that are usually synthesized experimentally in the absence of organics. The presence of a

widespread organic-rich matrix may thus explain the stabilization of the ACC layer as well as the clustering and submicrometer-size of the aragonite crystals, because organic molecules can promote the formation of numerous nucleation sites (36) and inhibit crystal growth by poisoning their surfaces (37). The widespread occurrence of EPS down to the nanometer-scale evidenced in this study may explain the micritic texture of Lake Van microbialites and more generally the micritic texture usually observed in carbonate microbialites (4). Some authors state that acidic polysaccharides inhibit carbonate precipitation, which instead occurs in EPS-poor areas where high concentrations of Ca and Mg have been released by the degradation of polysaccharides by heterotrophic bacteria (38). Others propose that decaying EPS transform into a highly organized template structure favoring calcium carbonate nucleation (39). Although polysaccharide degradation cannot be excluded, the presence of detectable amounts of EPS in Lake Van microbialites, including areas of extensive precipitation, is consistent with a promoter role for EPS in carbonate precipitation. The questions of whether the presence of EPS in Lake Van microbialites indicates that degradation by heterotrophic bacteria does not balance EPS production or that some molecules are more resistant than others to bacterial degradation and/or protected by mineral precipitation cannot be answered by this study. This pervasive association of organic polymers with aragonite supports a biogenic origin for microbialite carbonates, but the relatively low cell density observed shows that carbonates are not generally associated with detectable cells. Many ancient carbonates do not preserve clear evidence of the organisms responsible for their formation and hence their biogenicity has been questioned (11). Our observations reconcile these considerations with a biotic origin. Lake Van microorganisms and their pervasive associated polymers do impact mineral nucleation and/or growth of carbonate crystals in the highly oversaturated waters of the lake, producing clusters of nanobacteria-like aragonite crystals and leaving biosignatures in the mineralogy and in the associated organic matter of these deposits.

ACC has been observed around nanometer-sized rod-shaped calcite crystals surrounded by polysaccharides (40–41) and has also been recently described in mollusks and arthropods (42). Although ACC has not been described in microbial carbonates previously, its identification in Lake Van microbialites should stimulate a systematic search for this feature in carbonates precipitated in the presence of organic compounds. The presence of ACC is not a biosignature *per se* because ACC can be stabilized by abiotic impurities (43); however, its association with organic molecules may be an indicator of biogenicity. In that regard, the use of cryo-TEM to image single organic molecules in microbialites at very high spatial resolution would be an interesting approach to develop in the future. Moreover, the preservation of the organic-ACC layer after secondary mineralogical processes, such as transformation of aragonite to more stable carbonate phases (i.e., calcite, dolomite) that may affect older microbialites, is yet to be investigated.

Summary and Conclusions

Lake Van microbialites are composed of living and/or recently fossilized microbes and nanobacteria-like aragonite crystals, embedded together in a polysaccharide matrix. Our observations strongly suggest that the presence of this pervasive organic matrix, intimately associated with the aragonite crystals down to the nanometer scale, is responsible for the particular mineralogical features observed in Lake Van microbialites, i.e., clustered spherical aragonite crystals in the 30- to 100-nm size range, surrounded by a usually highly unstable ACC phase. The use of both STXM and TEM to characterize microbialites at the submicrometer scale provides a unique capability to detect viable or fossilized microbial cells and exopolymers in such deposits in the form of complex mixtures of organic functional groups. Although preservation of organic and mineralogical features of the type reported here heretofore has not been documented in ancient microbialites, understanding such signatures in modern microbialites is a prerequisite to their potential detection and use in determining the origin of ancient microbialites.

Methods

Samples were gently crushed in an agate mortar (see Fig. 12, which is published as supporting information on the PNAS web site). Powders were suspended for a few seconds in Milli-Q grade water, and one drop was deposited on the membrane of a lacey carbon-coated 200 mesh copper grid and dried in air. We did not detect either by STXM or by TEM any artifactual salt precipitation. STXM observations were performed at Advanced Light Source branch line 11.0.2.2 according to the procedures described in ref. 13. The synchrotron storage ring operated at 1.9 GeV and 200–400 mA stored current. A 150 lines per mm grating and 20-μm exit slit were used for carbon and nitrogen K-edge imaging and spectroscopy, providing a theoretical energy resolution of 100 meV. Energy calibration was accomplished by using the well resolved 3p Rydberg peak at 294.96 eV of gaseous CO_2 for the C K-edge. Calibration at the N K-edge was made by using the N 1s $\rightarrow \pi^*$ (401.1 eV) transition of atmospheric N_2 (44).

TEM observations were performed on a JEOL 2010F microscope operating at 200 kV and equipped with a field emission gun, a high-resolution UHR pole piece, and a Gatan GIF 200 energy filter. EELS analyses were performed according to the procedures described in ref. 14. EELS spectra were acquired by using a dispersion of 0.3 eV per channel to record spectra in the range 250–560 eV. The energy resolution was ≈1.3 eV as measured by the full width at half maximum of the zero-loss peak. The dwell time was optimized to acquire sufficient signal intensity and to limit beam damage. Spectra were corrected from plural scattering by using the Egerton procedure available with the EL/P program (Gatan).

We thank A. P. Hitchcock (McMaster University, Hamilton, ON, Canada) for providing carbon K-edge spectra for DNA, albumin, and sodium alginate. Bill Burkholder (Stanford University) kindly provided a *B. subtilis* strain. Microbialites were collected during a German–Turkish Geological Expedition to Lake Van (led by Stephan Kempe, Darmstadt), which was supported by the Deutsche Forschungsgemeinschaft. This work was supported by National Science Foundation Grant CHE-0431425 (Stanford EMSI) and by a grant from the Woods Institute for the Environment at Stanford University. The STXM studies were performed at the Advanced Light Source on the STXM end station (11.0.2.2) of the Molecular Environmental Science beam line (11.0.2), which is supported by the Division of Chemical Sciences, Geosciences, and Biosciences, Department of Energy Office of Basic Energy Sciences. The Advanced Light Source is supported by the Scientific User Facilities Division of the Department of Energy Office of Basic Energy Sciences.

1. Kempe, S., Kazmierczak, J., Landmann, G., Konuk, T., Reimer, A. & Lipp, A. (1991) *Nature* **349,** 605–608.
2. Kazmierczak, J. & Kempe, S. (2003) *Naturwissenschaften* **90,** 167–172.
3. López-García, P., Kazmierczak, J., Benzerara, K., Kempe, S., Guyot, F. & Moreira, D. (2005) *Extremophiles* **9,** 263–274.
4. Riding, R. (2000) *Sedimentology* **47,** 179–214.
5. Dupraz, C., Visscher, P. T., Baumgartner, L. K. & Reid, R. P. (2004) *Sedimentology* **51,** 745–765.
6. Kalkowsky, E. (1908) *Z. Dtsch. Geol. Ges.* **60,** 68–125.
7. Reid, R. P., Visscher, P. T., Decho, A. W., Stolz, J. F., Beboutk, B. M., Dupraz, C., Macintyre, I. G., Paerl, H. W., Pinckney, J. L., Prufert-Beboutk, L., *et al.* (2000) *Nature* **406,** 989–992.

8. Arp, G., Reimer, A. & Reitner, J. (2001) *Science* **292,** 1701–1704.
9. Bosak, T. & Newman, D. K. (2003) *Geology* **31,** 577–580.
10. Vasconcelos, C., McKenzie, J. A., Bernasconi, S., Grujic, D. & Tien, A. J. (1995) *Nature* **377,** 220–222.
11. Grotzinger, J. P. & Rothman, D. H. (1996) *Nature* **383,** 423–425.
12. Grotzinger, J. P. & Knoll, A. H. (1999) *Annu. Rev. Earth Planet. Sci.* **27,** 313–358.
13. Benzerara, K., Yoon, T. H., Tyliszczak, T., Constantz, B., Spormann, A. M. & Brown, G. E., Jr. (2004) *Geobiology* **2,** 249–259.
14. Benzerara, K., Menguy, N., Guyot, F., Vanni, C. & Gillet, P. (2005) *Geochim. Cosmochim. Acta* **69,** 1413–1422.
15. Maniloff, J. (1997) *Science* **276,** 1773–1776.
16. Boese, J., Osanna, A., Jacobsen, C. & Kirz, J. (1997) *J. Electron Spectrosc. Relat. Phenom.* **85,** 9–15.
17. Lawrence, J. R., Swerhone, G. D. W., Leppard, G. G., Araki, T., Zhang, X., West, M. M. & Hitchcock, A. P. (2003) *Appl. Environ. Microbiol.* **69,** 5543–5554.
18. Myneni, S. C. B. (2002) *Rev. Mineral. Geochem.* **49,** 485–579.
19. Gordon, M. L., Cooper, G., Morin, C., Araki, T., Turci, C. C., Kaznatcheev, K. & Hitchcock, A. P. (2003) *J. Phys. Chem. A* **107,** 6144–6159.
20. Decho, A. W. & Kawaguchi, T. (1999) *BioTechniques* **27,** 1246–1252.
21. Kawaguchi, T. & Decho, A. W. (2002) *Mar. Biotechnol.* **4,** 127–131.
22. Obst, M., Gasser, P., Mavrocordatos, D. & Dittrich, M. (2005) *Am. Mineral.* **90,** 1270–1277.
23. Ferris, F. G., Fyfe, W. S. & Beveridge, T. J. (1988) *Geology* **16,** 149–152.
24. Benzerara, K., Menguy, N., Guyot, F., Skouri, F., de Luca, G., Barakat, M. & Heulin, T. (2004) *Earth Planet. Sci. Lett.* **228,** 439–449.
25. Stolz, J. F., Feinstein, T. N., Salsi, J., Visscher, P. T. & Reid, R. P. (2001) *Am. Mineral.* **86,** 826–833.
26. Thompson, J. B., Schultze-Lam, S., Beveridge, T. J. & DesMarais, D. J. (1997) *Limnol. Oceanogr.* **42,** 133–141.
27. Westall, F. (2005) *Science* **308,** 366–367.
28. Arp, G., Reimer, A. & Reitner, J. (2003) *J. Sediment. Res.* **73,** 105–127.
29. Gautret, P., Camoin, G., Golubic, S. & Sprachta, S. (2004) *J. Sediment. Res.* **74,** 462–478.
30. Kühl, M., Fenchel, T. & Kazmierczak, J. (2003) in *Fossil and Recent Biofilms—A Natural History of Life on Earth*, eds. Krumbein, W. E., Paterson, D. M. & Zavarzin, G. A. (Kluwer Academic, Dordrecht, The Netherlands), pp. 77–102.
31. Kazmierczak, J., Kempe, S. & Altermann, W. (2004) in *The Precambrian Earth: Tempos and Events*, eds. Eriksson, P. G., Altermann, W., Nelson, D. R., Mueller, W. U. & Catuneanu, O. (Elsevier, Amsterdam), pp. 545–564.
32. Rougeaux, H., Guezennec, M., Che, L. M., Payri, C., Deslandes, E. & Guezennec, J. (2000) *Mar. Biotechnol.* **3,** 181–187.
33. Decho, A. W. (2000) *Continental Shelf Res.* **20,** 1257–1273.
34. Kawaguchi, T. & Decho, A. W. (2000) *Prep. Biochem. Biotechnol.* **30,** 321–330.
35. Aizenberg, J., Lambert, G., Weiner, S. & Addadi, L. (2002) *J. Am. Chem. Soc.* **124,** 32–39.
36. Grassmann, O. & Lobmann, P. (2004) *Biomaterials* **25,** 277–282.
37. Manoli, F. & Dalas, E. (2002) *J. Mater. Sci. Mater. Med.* **13,** 155–158.
38. Arp, G., Reimer, A. & Reitner, J. (1999) *Eur. J. Phycol.* **34,** 393–403.
39. Défarge C., Trichet, J., Jaunet, A. M., Robert, M., Tribble, J. & Sansone, F. J. (1996) *J. Sediment. Res.* **66,** 935–947.
40. Benzerara, K., Menguy, N., Guyot, F., Dominici, D. & Gillet, P. (2003) *Proc. Natl. Acad. Sci. USA* **100,** 7438–7442.
41. Benzerara, K., Yoon, T.-H., Menguy, N., Tyliszczak, T. & Brown, G. E., Jr. (2005) *Proc. Natl. Acad. Sci. USA* **102,** 979–982.
42. Becker, A., Bismayer, U., Epple, M., Fabritius, H., Hasse, B., Shi, J. M. & Ziegler, A. (2003) *J. Chem. Soc. Dalton Trans.* **4,** 551–555.
43. Raz, S., Weiner, S. & Addadi, L. (2000) *Adv. Mater.* **12,** 38–42.
44. Sodhi, R. N. S. & Brion, C. E. (1984) *J. Electron Spectrosc. Rel. Phenom.* **34,** 363–372.